Journal of Neuroimmunology 264 (2013) 71–83

Contents lists available at ScienceDirect

Journal of Neuroimmunology

journal homepage: www.elsevier.com/locate/jneuroim

Elevated CD3$^+$ and CD8$^+$ tumor-infiltrating immune cells correlate with prolonged survival in glioblastoma patients despite integrated immunosuppressive mechanisms in the tumor microenvironment and at the systemic level ☆

Justyna Kmiecik [a], Aurélie Poli [a,b], Nicolaas H.C. Brons [b], Andreas Waha [c], Geir Egil Eide [d,e], Per Øyvind Enger [f], Jacques Zimmer [b], Martha Chekenya [a,g,*]

[a] Department of Biomedicine, University of Bergen, Jonas Lies vei 91, 5009 Bergen, Norway
[b] Laboratoire d'Immunogénétique-Allergologie, CRP-Santé, 84 Val Fleuri, L-1526, Luxembourg
[c] Department of Neuropathology, University Hospital, Bonn, Germany
[d] Centre for Clinical Research, Haukeland University Hospital, Jonas Lies vei 91, 5021 Bergen, Norway
[e] Department of Global Public Health and Primary Care, University of Bergen, Kalfarveien 31, 5020 Bergen, Norway
[f] Department of Neurosurgery, Haukeland University Hospital, 5021 Bergen, Norway
[g] Department of Clinical Dentistry, University of Bergen, Årstadveien 19, 5009 Bergen, Norway

ARTICLE INFO

Article history:
Received 5 June 2013
Received in revised form 12 August 2013
Accepted 22 August 2013

Keywords:
GBM
Tumor infiltrating cells
Regulatory T cells
Antigen presenting cells

ABSTRACT

We characterized GBM patients' tumor and systemic immune contexture with aim to reveal the mechanisms of immunological escape, their impact on patient outcome, and identify targets for immunotherapy. Increased CD3$^+$ T-cell infiltration was associated with prolonged survival independent of age, MGMT promoter methylation and post-operative treatment that implies potential for immunotherapy for GBM. Several mechanisms of escape were identified: within the tumor microenvironment: induced CD8$^+$CD28$^-$Foxp3$^+$ T_{regs} that may tolerize antigen presenting cells, elevated CD73 and CD39 ectonucleotidases that suppress T-cell function, and at the systemic level: elevated IL-10 levels in serum, diminished helper T-cell counts, and upregulated inhibitory CTLA-4.

1. Introduction

Glioblastoma (GBM) is the most frequent and malignant brain tumor classified as grade IV by the World Health Organization (Louis et al., 2007) and accounts for 52% of all gliomas. The current treatment combines surgical debulking with chemotherapy and radiotherapy, however, the patients' survival remains very low (Stupp et al., 2005), emphasizing the need for continued search for novel and effective therapies. Identifying molecular markers that associate with beneficial patient survival is critical for highlighting important biological processes involved in disease progression and may guide the search for innovative therapies.

For a long time the brain was considered an immune privileged organ due to the presence of the blood brain barrier (BBB), lack of lymphatic drainage and of professional antigen presenting cells (APCs). Therefore, brain tumors were considered protected from immune surveillance. However, recent investigations showed that activated immune cells can cross the BBB (Becher et al., 2000; Sehgal and Berger, 2000; Alter et al., 2003; Prendergast and Anderton, 2009), which is also often disrupted at the tumor site, and that microglia can act as resident APCs (Becher et al., 2000; Yang et al., 2010a). Thus, the role of the immune system in brain cancer has become a subject of intensive study. It has been shown, that the immune cells perform anti-tumor surveillance and display potential for killing the tumor cells (Costello et al., 2002; Tang et al., 2005; Carpentier and Meng, 2006; Ueda et al., 2007). However, GBM develops multiple escape mechanisms, such as expression of inhibitory molecules (Rouas-Freiss et al., 2005; Gomez and Kruse, 2006; Malmberg and Ljunggren, 2006; Zhang, 2010) and release of soluble immunosuppressive factors (Zou et al., 1999; Gomez and Kruse, 2006; Malmberg and Ljunggren, 2006). Moreover, the role of the immune system in cancer is ambiguous, as there exist immune cell subpopulations that promote tumor progression (de Visser et al., 2006; Fecci et al., 2006; Wang, 2008; Ostrand-Rosenberg and Sinha, 2009) and that are thought to be induced by the tumor cells. There is no consensus on the impact of tumor immune infiltration on the patient's overall outcome, nor are the mechanisms involved in the patients' systemic response to the tumor delineated.

* Corresponding author at: Translational Cancer Research Group, Jonas Lies vei 91, N-5009 Bergen, Norway. Tel.: +47 55586380; fax: +47 55586360.
E-mail address: martha.chekenya@biomed.uib.no (M. Chekenya).

0165-5728/$ – see front matter © 2013 The Authors. Published by Elsevier B.V. All rights reserved.
http://dx.doi.org/10.1016/j.jneuroim.2013.08.013

In the present study we characterized the immune profile of GBM patients and identified several coordinated mechanisms of tumor-driven immune suppression. A substantial number of functional studies describing tumor-immune interactions focused only on particular subpopulations and markers. The aim of our work was to broadly investigate the immune contexture of GBM patients both within the tumor microenvironment and at the systemic level. We highlight the coordinated anti-tumor immune responses and tumor-mediated immune escape mechanisms. Our results demonstrated a significant positive correlation of increased $CD3^+$ and $CD8^+$ cellular infiltration into the tumor with improved patient survival. The major mechanisms of tumor immune escape in GBM patients were (1) induction of $CD8^+CD28^-Foxp3^+$ T_{regs}, that could mediate the tolerization of APCs by upregulating immunoglobulin-like transcript (ILT) inhibitory receptors and downregulating CD80, CD86 and CD40 costimulatory molecules (Fecci et al., 2006) and high surface expression of CD73 that could lead to T-cell suppression (Jeffes et al., 1993; Purdy and Campbell, 2009; Hausler et al., 2011). Comparison between the GBM patients' and healthy donors' PBMCs and plasma also revealed systemic immunosuppression. Thus, detailed characterization of the patients' immune status is required for design of appropriate immunotherapy for GBM.

2. Materials and methods

2.1. Blood and tumor material

Patients' blood and GBM biopsies were obtained during surgical resections performed at the Haukeland University Hospital, Norway, between 2009 and 2011. The patients gave their written informed consent and the study was approved by the Norwegian regional Helse-Vest ethical board. Parts of the tumor were formalin fixed and paraffin embedded (FFPE). H&E-stained sections were prepared to define representative tumor regions and the neuropathologists at the department of pathology, Gades Institute, Haukeland University Hospital routinely confirmed GBM diagnosis according to the World Health Organization (WHO) classification (Louis et al., 2007). Furthermore, patients diagnosed with GBM had routine follow-up with MRI interpreted by neuroradiologists at the department of radiology, Haukeland University Hospital, as part of their routine management. Eligibility criteria included availability of follow-up data, less than 50% necrosis in the sample, and only biopsies obtained at primary diagnosis were included. Clinical information was obtained by reviewing the medical records, and death certificates/registers. Patients were followed-up from the date of operation until death or December 2012. The median follow-up of the seven patients that were alive was 30 months, range 23–39 months. All patients were treated by surgery, radiotherapy and/or chemotherapy and survival determined as the time elapsed from the date of surgery to the date of death.

Part of the fresh tissue was dissociated by use of Neural Tissue Dissociation Kit as recommended by the manufacturer (Miltenyi Biotec, Bergisch Gladbach, Germany). Cell suspension was frozen in 10% DMSO (Sigma, St. Louis, MO) and 10% fetal bovine serum (FBS) (PAA, Pasching, Austria) solution according to standard protocol. Peripheral blood was collected using BD Vacutainer® CPT™ Cell Preparation Tube with Sodium Citrate (BD Biosciences, Franklin Lakes, NJ) and Peripheral Blood Mononuclear Cells (PBMCs) were isolated and frozen as above. Patients' plasma was stored at −20 °C., PBMCs and plasma were isolated from age and gender matched healthy donors (Table S1) using the same method.

2.2. Immunohistochemistry

FFPE tissue was subjected to immunohistochemistry using the avidin–biotin–peroxidase complex method according to the manufacturer's protocol (Vectastain, Vector laboratories, Burlingame, CA). FFPE sections from 65 patients were immunolabeled with rabbit anti-human CD3 (Dako, Glostrup, Denmark), mouse anti-human CD4 (Novocastra™ Leica Microsystems GmbH, Wetzlar, Germany) and mouse anti-human CD8α (Dako) primary antibodies according to standard protocols. Human tonsil tissue was used for positive control and staining with irrelevant primary antibody (MOC-31, Santa Cruz Biotechnology, Santa Cruz, CA) as negative control. $CD3^+$ cells were quantified by morphometry and the result presented as percentage of total number of cells. Area fractions (%) of $CD4^+$ and $CD8^+$ cells were quantified on 89,400 μm^2 field of view (magnification 400×), minimum of 4 fragments, representing hot spots, per each section and were analyzed, using NIS-Elements BR v4 software (Nikon).

2.3. Bisulfite treatment and MGMT methylation analysis

For the analysis of MGMT promoter methylation, DNA was extracted from snap-frozen tumor tissue using the QIAamp DNEasy mini kit (Qiagen, Hilden, Germany). Bisulfite conversion was conducted as previously described (Mikeska et al., 2007).

Table 1
Fluorochrome-conjugated antibodies used for PBMCs and GBM phenotyping. The antibodies were purchased from: BD Biosciences, Franklin Lakes, NJ; Invitrogen, Paisley, UK; eBioscience San Diego, CA; BioLegend, San Diego, CA; ImmunoTools (Friesoythe, Germany); and R&D Systems Abingdon, UK.

Antibody	Manufacturer
PE-CD152 (CTLA-4)	BioLegend
PE-TexasRed-CD56	Invitrogen
PerCP-Cy5.5-CD25	eBioscience
PE-Cy7-CD4	BD Biosciences
Alexa647-CD127	BD Biosciences
Alexa700-CD62L	BioLegend
Alexa750-CD8	Invitrogen
V450-CD8	BD Biosciences
Pacific orange-CD45	Invitrogen
PE-HLA-A,B,C	BD Biosciences
PE-Dy647-CD19	ImmunoTools
PerCP-Cy5.5-CD45	BD Biosciences
PE-Cy7-CD31	BioLegend
PE-Dy747-CD4	ImmunoTools
APC-CD25	BD Biosciences
V450-CD80	BD Biosciences
V450-CD86	BD Biosciences
V450-CD27	BD Biosciences
V450-CD40	BD Biosciences
V450-CD73	BD Biosciences
Pacific Blue™-CD154	BioLegend
V450-CD31	BD Biosciences
V450-CD56	BD Biosciences
V500-CD3	BD Biosciences
Brilliant Violet 570™-CD4	BioLegend
FITC-CD28	BD Biosciences
Alexa Fluor® 488-MICA	R&D Systems
FITC-CD62L	BD Biosciences
FITC-ILT2	R&D Systems
FITC-ILT3	R&D Systems
FITC-ILT4	R&D Systems
FITC-CD95	BD Biosciences
FITC-CD16	BD Biosciences
FITC-TCR Vα24-Jα18 (iNKT cell)	BioLegend
PE-MICB	R&D Systems
PE-CD70	BD Biosciences
PE-CD39	BioLegend
PE-HLA-G	eBioscience
PE-HLA-E	eBioscience
PE-CD178 (Fas-L)	BioLegend
PE-NKG2D	R&D Systems
PE-CD1d	BioLegend
PE-CF594-CD14	BD Biosciences
PerCP-Cy5.5-CD45	BD Biosciences
PE-Cy7™-CD8	BD Biosciences

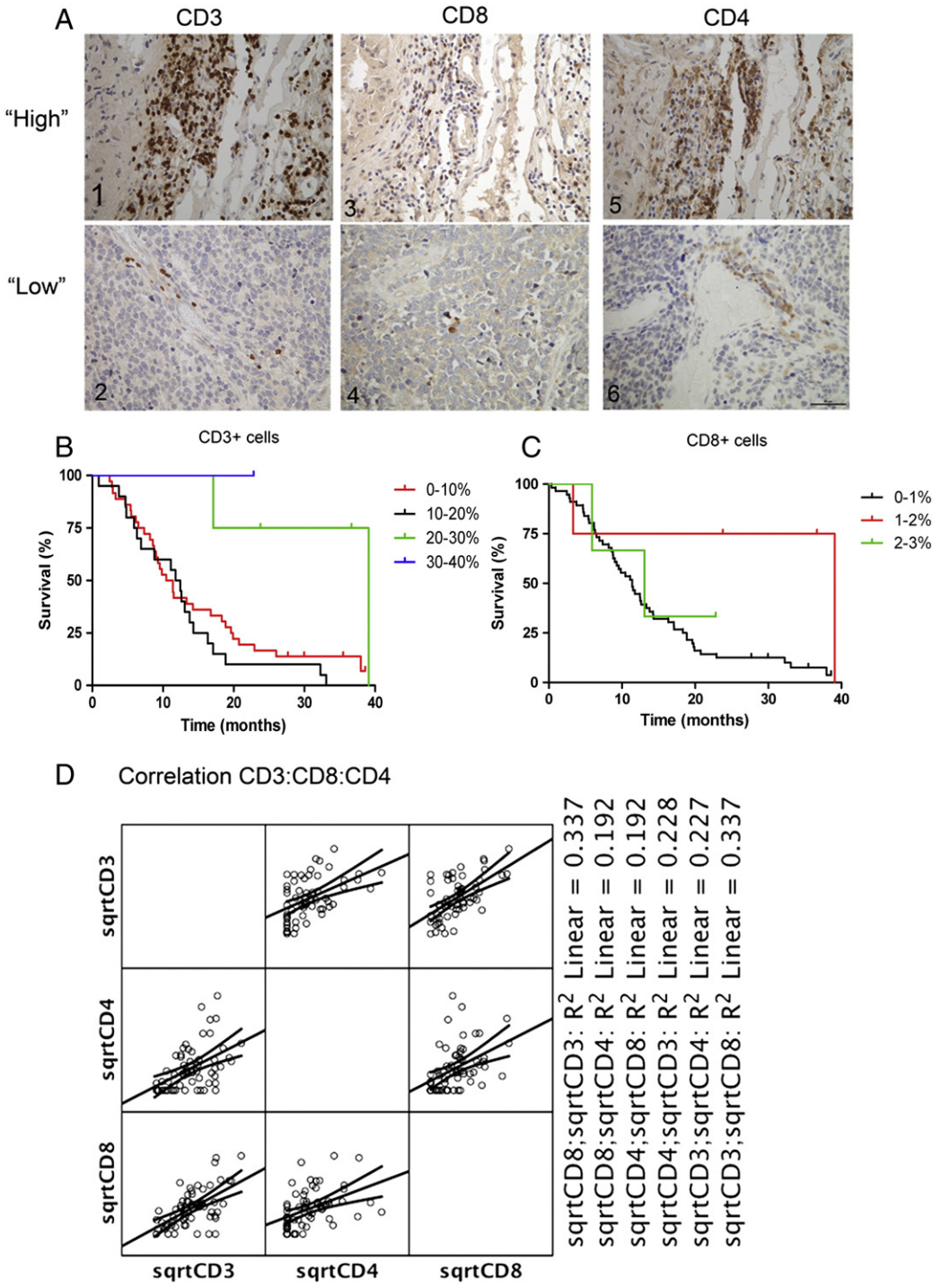

Fig. 1. Immune cell infiltration into the tumor microenvironment. A. Representative IHC staining of GBM biopsy: 1, 2: CD3 staining — patients with high and low numbers of CD3 positive cells; 3, 4: CD8 staining — patients with high and low numbers of CD8 positive cells; 5, 6: CD4 staining — patients with high and low numbers of CD4 positive cells; B and C. Kaplan–Meier survival curves of $CD3^+$ and $CD8^+$ cell infiltration with patients' % survival time in months. D. Covariance of $CD3^+$, $CD8^+$ and $CD4^+$ cells. Magnification 400×, scalebar in A6 50 μm.

2.4. Flow cytometry

2.4.1. PBMCs and GBM tumor phenotyping

PBMCs/GBM cells were thawed, counted, and washed with PBS containing 0.5% BSA and 2% mouse serum. Surface stainings were performed according to standard protocol with different combinations of fluorochrome-conjugated mouse anti-human antibodies present in Table 1. Proper isotype controls were used to exclude unspecific antibody binding. PBMCs were stained with LIVE/DEAD® Fixable Blue Dead Cell Stain Kit (Invitrogen, Paisley, UK) and GBM cells with LIVE/DEAD® Fixable Near-IR Dead Cell Stain Kit (Invitrogen) according to manufacturer's instructions. PBMCs were then fixed and permeabilized with Foxp3/Transcription Factor Staining Buffer Set (eBioscience San Diego, CA) and stained with eFluor450-conjugated anti-human Foxp3 (eBioscience) and PE-CD152 (CTLA-4) (BioLegend, San Diego, CA) according to manufacturer's recommendations. GBM cells were fixed and permeabilized with Cytofix/Cytoperm (BD Biosciences), washed with Perm/Wash buffer (BD Biosciences) containing 2% mouse serum and stained for intracellular markers with PE-CD152 (CTLA-4) (BioLegend) and PE-Foxp3 (BD Biosciences). For better

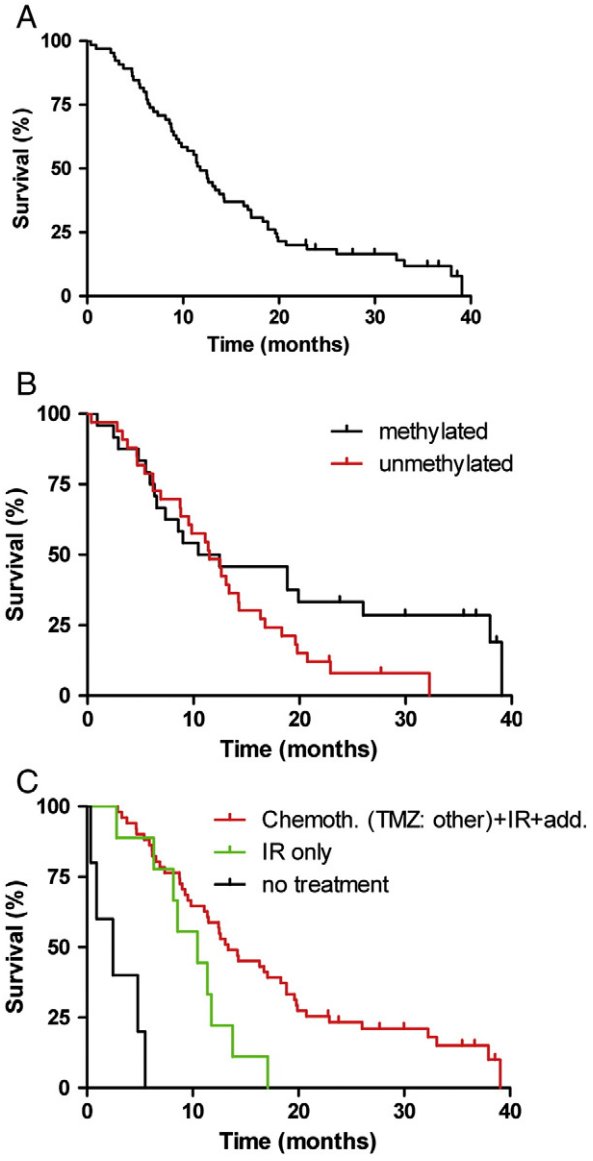

Fig. 2. (A) Kaplan–Meier % survival curves and observation time in months of the whole patient group (n = 65). Median survival with censored patients, median ± SEM (95% CI) 11.7 ± 0.8(10–13.4). (B) Cumulative survival by MGMT status (p = 0.093). (C) Kaplan–Meier % survival by post-operative treatment (p = 0.0001).

discrimination between nucleated cells and debris in GBM samples, each sample was stained with Hoechst (Sigma) or TO-PRO®-3 iodide (Invitrogen) for 10 min or 2 min, respectively, before data acquisition. Data were acquired using BD FACSAria and BD LSRFortessa flow cytometers and data analyzed with BD FACSDiva Software v6.2 (BD Biosciences Franklin Lakes, NJ).

2.4.2. Gating strategy applied to PBMC phenotyping

Debris and dead cells were gated based on size on FSC vs. SSC channels and Live/Dead staining and excluded from the analysis. Doublets were excluded based on SSC-A vs. SSC-H plot. T-cell population was gated based on the FSC and SSC parameters and surface expression of CD3. Two main populations of T-cells were gated: $CD4^+$ (helper T-lymphocytes, T_h) and $CD8^+$ (cytotoxic T-lymphocytes, CTLs) and $CD4^+$ (helper T-lymphocytes, T_h). Naturally occurring regulatory T-cells (T_{regs}) were defined as $CD4^+CD25^{high}Foxp3^+$ cells (Fig. 3H). As additional markers confirming this identification, CD152 and CD127 were used (Hartigan-O'Connor et al., 2007) (Fig. 3H).

2.4.3. Gating strategy applied to GBM biopsy phenotyping

Dead cells were excluded from the analysis based on Live/Dead staining (Fig. S1C). We used Hoechst or TO-PRO®-3 iodide staining on fixed and permeabilized cells in addition to FSC and SSC parameters to include in our analysis only nucleated cells (Fig. S1B). Doublets were excluded based on SSC-A vs. SSC-H plot. Tumor infiltrating-immune cells were defined as $CD45^+$ cells (Fig. S1C). The population of CD45-cells was investigated for the presence of endothelial cells based on CD31 expression. Only 2.288% ±0.9889 of all $CD45^-$ cells expressed CD31; therefore, we defined the CD45 negative fraction as tumor cell enriched. In each staining within $CD45^+$ cells, the following subpopulations of immune cells were distinguished: T-cells gated as small (FSC parameter), $CD3^+$, $CD8^+$ (CTLs) and $CD4^+$ (T_h) events (Fig. S1F, G, H). Monocytes/macrophages/dendritic cells were gated based on FSC and SSC parameters (Fig. S1F) and henceforth designated antigen presenting cells (APCs) in the text. In additional stainings, B-cells were defined as small, $CD3^-CD19^+$ cells, NK cells gated as $CD3^-CD14^-CD56^+$ cells and 3 different T_{regs} subpopulations defined as $CD4^+CD25^{high}Foxp3^+$, $CD8^+CD28^-Foxp3^+$, and $CD8^+CD25^+Foxp3^+$. We also examined T-cell population for the expression of TCR Vα24-Jα18 — a marker for type I natural killer T-cells.

2.4.4. Plasma analysis — Cytometric Bead Array (CBA)

Concentration of 16 proteins was measured with CBA technique in plasma samples from GBM patients and in age- and gender-matched healthy donors. We used Human Soluble Protein Master Buffer Kit (BD Biosciences), Human Flex Sets according to the manufacturer's protocol (BD Biosciences) listed in Table 4 and Human TGF-β1 Single Plex Flex Set (BD Biosciences). Data were acquired on BD Canto and BD LSRFortessa flow cytometers and analyzed with FCAP Array Software (Soft Flow Inc., Pecs, Hungary).

2.5. Statistics

Patient survival was estimated using the Kaplan–Meier method (Kaplan and M.P., 1958) and compared between groups with the log rank test (Mantel, 1966). Univariate analyses were performed to identify variables with significant prognostic impact ($p < 0.05$) and, these variables were further included in the Cox proportional hazards model. Backward stepwise selection was applied to select variables to adjust for effects of potential confounding variables including age (0–10, 10–20, 20–30, 30–40, 40–50, 50–60, 60–70, 70–80 years) and post-operative treatment, CD3 (grouped 0–10, 10–20, 20–30, 30–40), CD8 and CD4 (grouped 0–1, 1–2, 2–3) gender and MGMT as categorical variables. To compare the patient and healthy donor group the non-parametric Wilcoxon signed rank test was used. When comparing more than two cell populations within patient GBM or between patients and donors we used One-Way ANOVA tests (Friedman and Kruskal–Wallis, respectively). In all analyses probability values less or equal to 0.05 were considered significant. Descriptive statistics are reported as mean, mean ± standard error of the mean (SEM). All statistical analyses were performed with the (SPSS) v11.0 software.

3. Results

3.1. Increased tumor infiltration of $CD3^+$ and $CD8^+$ cells correlates with prolonged patient survival

Analysis of CD3, CD4 and CD8 expressing cells in 65 GBM biopsies revealed a great heterogeneity in the amounts and their spatial localization, both between and within the patients' tumors (Fig. 1A). In some cases the immune cells were localized in hotspots in the vicinity of blood vessels and/or infiltrated the entire tumor (Fig. 1A). To determine the impact of the degree of infiltration of immune cells on tumor progression, we quantified the $CD3^+$, $CD4^+$ and $CD8^+$

immune cells in the 65 unassigned GBM biopsies and correlated the expression with the patients' outcome. The mean and the median survival of the patient population were 19.6 ± 1.8 and 11.7 ± 0.8 months respectively (Fig. 2A). Mean and median survival of females were 13.8 ± 2 and 9.5 ± 1.8 months respectively, compared to males 16.4 ± 1.9 and 9.8 ± 1.4 months respectively, (Table 2). In univariate analyses, gender had no significant impact on patients' survival, Log Rank (Mantel–Cox) Chi-square 0.77, df = 1, p = 0.37. Although methylation of the methyl guanine DNA methyltransferase (MGMT) gene promoter is established as predictive of response to temozolomide chemotherapy (Hegi et al., 2005; Stupp et al., 2009), reports of its prognostic role have been variable (Costa et al., 2010). In our material, MGMT promoter methylation was not significantly associated with patient survival, Log Rank (Mantel–Cox) Chi-square 2.82, df = 1, p = 0.093 (Fig. 2B and Table 2). Preoperative treatment with steroids had no effect on outcome, Log Rank, Chi-square 5.196, df = 4, p = 0.268 (Table 2). Age at diagnosis was a significant prognostic factor, Log Rank (Mantel–Cox) Chi-square 14.11 df = 6, p = 0.028. Post-operative treatment had a significant effect on overall survival, p = 0.0001, (Table 2). Quantification of $CD3^+$ immune cell infiltrates revealed a correlation of increased $CD3^+$ T-cell infiltration with longer survival, Log Rank, Chi-square 9.58, df = 3, p = 0.022, (Fig. 1B). There was a trend for CD8, Log Rank, Chi-square 5.56 df = 2, p = 0.062, and no association of $CD4^+$ immune infiltrates with overall patient survival, Log Rank, Chi-square 1.28, df = 2, p = 0.52. To investigate whether increased $CD3^+$ and $CD8^+$ cells were independent prognostic factors we corrected for age, MGMT status and post-operative treatment using backward, stepwise Cox regression analysis. Increased $CD8^+$ immune cell infiltrates were then associated with longer survival independent of age at diagnosis, Chi-square 4.87, df = 1, p = 0.027. Increased $CD3^+$ T cell infiltration was associated with longer survival independent of age, and post-operative treatment, p = 0.027. Moreover, $CD3^+$ immune infiltrates were significantly correlated with $CD8^+$ cells, (Pearson correlation 0.579, p < 0.0001, n = 59) and with $CD4^+$ cells, (Pearson correlation 0.47, p < 0.0001 n = 59), (Fig. 1D and Table S2).

Table 2
Survival, patient clinical parameters and statistical significance.

Variable	n	Median survival ± SEM (months)	95% CI (months)	p-Value Log Rank Mantel–Cox	p-Value Cox
Gender					0.37
Males	35	13.0 ± 1.4	(10.3–15.8)		
Females	30	9.5 ± 1.8	(5.8–13.1)		
Age				**0.028**	**0.010**
<10	1	12.6			
20–30	2	12.4			
30–40	5	18.3 ± 1.7	(14.9–21.7)		
40–50	7	18.8 ± 13.1	(0–44.6)		
50–60	17	16.3 ± 2.5	(11.3–21.3)		
60–70	26	8.7 ± 22	(4.2–13.2)		
70–80	7	8.5 ± 3.1	(2.4–14.6)		
MGMT				0.093	
Unmehtylated	33	11.5 ± 1.5	(8.3–14.6)		
Methylated	24	10.4 ± 1.5	(0.5–30.3)		
Pre-Op steroids				0.268	
Unknown	14	12.6 ± 3.0	(6.6–18.5)		
1 day	14	12.4 ± 0.6	(11.13–13.7)		
2–7 days	19	9.5 ± 2.3	(4.9–14.1)		
8–14 days	11	17.0 ± 3.6	(9.8–24.2)		
Over 14 days	7	6.5 ± 0.4	(5.6–7.3)		
CD4					
<10%	56	11.3 ± 1.2	(8.8–13.8)	0.526	
10–20%	4	12.4 ± 4.4	(3.8–21.1)		
20–30&	2	6.5			
CD8				0.062	**0.027**
<1%	56	11.3 ± 1.2	(9.0–13.7)		
1–2%	4	39.0 ± 0			
2–3%	3	13.0 ± 5.8	(1.5–24.5)		
CD3				**0.022**	**0.024**
<10%	36	6.5 ± 1.7			
10–20%	20	5.9 ± 1.4			
20–30%	4	17.1			
>30%	1				
Post-op treatment					**0.0001**
None	5	2.4 ± 1.6	(0–5.7)		
IR only	9	10.4 ± 2.9	(4.9–16.0)		
Chemo + IR (TMZ ± other + radiation + additional)	51	13.3 ± 1.9	(9.4–17.2)		

The p-values in bold are those that are statistically significant.
[a] Median survival and 95% confidence interval, in months.
[b] Patient age was used as continuous variable for the Cox-regression model.

3.2. Patients' T cells present a suppressed phenotype within the tumor microenvironment and a moderate immunosuppression was observed at the systemic level

To identify the phenotype of the tumor infiltrating immune cells impacting patients' outcome, 8 patients' biopsies randomly selected from the original cohort were dissociated and single cells analyzed using multicolor flow cytometry. We compared proportion and phenotype of tumor infiltrating T-cell subpopulations with paired patients' peripheral T-cells and with 9 gender and age matched healthy donors' T-cells. First, we observed that the proportion of T_h in patients' blood was significantly diminished compared to normal donor (45.28% ± 7.20 and 65.68% ± 2.10 of $CD3^+$ cells, respectively, p = 0.0005, Fig. 3B and Table 3) and there was a tendency for further diminution within the tumor microenvironment (29.43% ± 7.20 of $CD3^+$ cells, Fig. 3B and Table 3). However, no significant differences in the percentage of CTL cells were found when we compared the blood of patients to donors and GBM biopsy (Fig. 3A and Table 3). No significant difference was observed in the expression of the co-stimulatory receptor CD28 (Fig. 3C, D and Table 3) and L-selectin CD62L (Fig. 3E, Table 3) in patients' and donors' peripheral T_h cells and CTLs, while it was down regulated in tumor infiltrating T_h cells and CTLs when compared to patients' peripheral T cells (Fig. 3C, D, E and Table 3). Moreover, tumor infiltrating CTLs displayed decreased expression of the adhesion molecule CD56 when compared to patients' peripheral CTLs, while no difference was observed comparing patients' vs. donors' peripheral CTLs (Fig. 3F, Table 3). Significantly more of patients' peripheral T_h cells compared to donors' expressed the inhibitory receptor CTLA-4, however, there was a trend for diminution within the tumor infiltrating T_h (Fig. 3G, Table 3). Furthermore, we investigated the presence of T_{regs} in 9 donors' and patients' peripheral blood and in 5 paired GBM biopsies. The naturally-occurring $CD4^+CD25^{high}Foxp3^+$ T_{regs} were not detected among the tumor infiltrating immune cells in our GBM patients (data not shown) and no difference was found in the proportions of these T_{regs} within patients' vs. donors' peripheral T cells (Fig. 3I and Table 3). However, in 60% (3/5) of the patients, $CD8^+CD28^-Foxp3^+$ T_{regs} were identified and represented 2.08% ± 0.99 of all T-cells (Fig. 3J). They were not detected in the blood of both patients and controls. In addition, we examined the GBM biopsies for the presence of NK and B cells. They were not very abundant and represented 2.11% ± 0.54 and 0.66% ± 0.27 (n = 8) of all tumor infiltrating immune cells, respectively. Within all patients, NK cells were predominantly $CD56^{dim}CD16^{negative}$ (Fig. 3K) and 57.45% ± 12.05 expressed the activating receptor NKG2D (Fig. 3K). Six patients' biopsies were analyzed for the presence of type I natural killer T-cells. However, they constituted only 1.13% ± 0.65 of all T-cells (data not shown).

3.3. Tumor infiltrating macrophages/microglia present immunotolerized phenotypes

The tumor-induced population of $CD8^+CD28^-Foxp3^+$ T_{regs} detected in our patients' biopsies has been reported to mediate immune

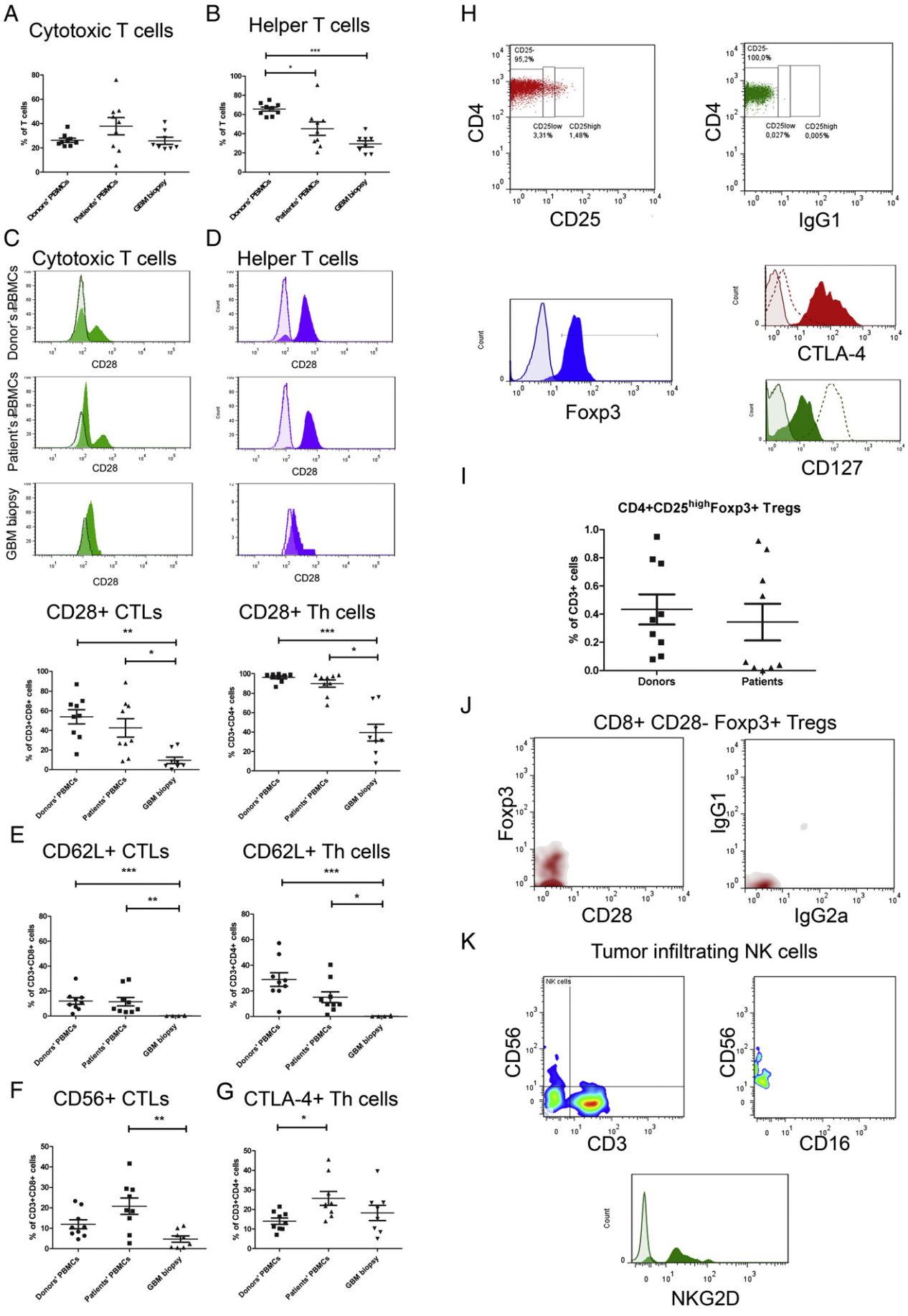
A
Cytotoxic T cells
% of T cells
Donors' PBMCs
Patients' PBMCs
GBM biopsy
B
Helper T cells
C
Cytotoxic T cells
Donor's PBMCs
Patient's PBMCs
GBM biopsy
CD28
D
Helper T cells
CD28+ CTLs
% of CD3+CD8+ cells
CD28+ Th cells
% of CD3+CD4+ cells
E
CD62L+ CTLs
CD62L+ Th cells
F
CD56+ CTLs
G
CTLA-4+ Th cells
H
CD25-
95,2%
CD25low
3,31%
CD25high
1,48%
CD4
CD25
CD25-
100,0%
CD25low
0,027%
CD25high
0,005%
IgG1
Foxp3
Count
CTLA-4
CD127
I
CD4+CD25highFoxp3+ Tregs
% of CD3+ cells
Donors
Patients
J
CD8+ CD28- Foxp3+ Tregs
Foxp3
CD28
IgG1
IgG2a
K
Tumor infiltrating NK cells
NK cells
CD56
CD3
CD16
NKG2D

tolerization by up regulating the expression of inhibitory receptors: immunoglobulin-like transcripts 2, 3, and 4 (ILT2, -3, -4) and down regulating the expression of co-stimulatory molecules CD40, CD80 and CD86 on APCs (Wang, 2008). Therefore, we investigated the phenotype of tumor infiltrating APCs (mainly macrophages/microglia). Remarkably, these cells represented the major subtype of immune cells in the tumor microenvironment, constituting 53.50% ±4.30 (n = 8) of all immune cells (Suppl Fig. 1 shows gating strategy). 13.21% ±6.90 of APCs expressed CD4 and 21.49% ±4.16 expressed CD8 (n = 8, Fig. 4A and B). Substantial proportions of APCs were positive for ILT2, ILT3 and ILT4 (38.60% ±6.79; 43.25% ±6.35 and 28.79% ±4.66, respectively, n = 8, Fig. 4A and C). Moreover, these cells highly expressed HLA-G and HLA-E (40.34% ±5.93 and 61.11% ±4.72 of positive cells, respectively, n = 8, Fig. 4A and D) that are ligands for ILTs and NKG2A inhibitory receptor. Only small proportions of APCs expressed CD40, CD80 and CD86 (12.61% ±3.37, 4.14% ±2.38 and 15.73% ±4.12, respectively, n = 8, Fig. 4E and F). On the other hand, we detected a proportion of APCs expressing MHC class I – related chains A and B (MICA and MICB) – ligands for the NKG2D activating receptor (26.53% ±6.60 and 8.39% ±2.71 of all APCs, n = 8, respectively, Fig. 4E and G). Interestingly, nearly half of APCs (46.58% ±9.54, n = 8, Fig. 4E and H) expressed NKG2D.

3.4. Tumor infiltrating immune cells display impaired expression of co-stimulatory molecules

Additionally, we investigated the tumor infiltrating immune cells for expression of co-stimulatory ligands and receptors important for immune function. Immune response can be stimulated upon binding of CD40 expressed on APCs to its ligand CD154 expressed on activated T-cells and some NK cells (Foy et al., 1996; Jyothi and Khar, 2000). Our results show that in GBM biopsies 12.61% ±3.37 of APCs are $CD40^+$ and all T-cells are $CD154^-$ (n = 8, Fig. 5A). We investigated the expression of CD27 and its ligand CD70 that are also involved in immune modulation (Garcia et al., 2004). In our patient cohort, 33.49% ±4.00 of T-cells expressed CD70 whereas all T-cells were $CD27^-$ (n = 8, Fig. 5B). Almost no T-cells expressed FasL (0.39% ±0.27 $FasL^+$ of all T-cells, n = 8, data not shown). However, the majority of CTLs (82.75% ±3.30, n = 8, Fig. 5C) expressed NKG2D.

3.5. Tumor integrated mechanisms of immune escape vs. potential immunogenicity

We analyzed the tumor cells for the expression of molecules potentially involved in immune escape or immunogenicity. Our results show that in all patients analyzed, the majority of tumor cells are positive for HLA-A,B,C (93.26% ±1.85, n = 8, Fig. 6A and B). On the other hand, only small proportions of tumor cells expressed HLA-G and HLA-E (0.538% ±0.27 and 6.23% ±3.50, respectively, n = 8, Fig. 6A and B). The tumor cells failed to express MICB and CD70 — ligands for activating receptors present on immune cells. However, a proportion of tumor cells were MICA positive (24.53% ±8.78, n = 8, Fig. 6A and C). We also analyzed tumor cells for the expression of Fas and FasL. All tumor cells were negative for FasL while 21.54% ±4.37 expressed Fas (n = 8, Fig. 6A and D). Additionally, we examined both tumor and tumor infiltrating immune cells for the expression of CD39 and CD73 ectonucleotidases that have been described to mediate immunosuppression of T cells (Hausler et al., 2011). In our patients, larger proportions of tumor cells were positive for CD73 compared to APCs and T-cells (33.49% ±5.31 vs. 8.150% ±2.83 and 3.54 ± 0.90, respectively, n = 8, $p > 0.05$ and $p = 0.0099$, respectively, Fig. 6E). Contrasting results were obtained for the CD39 molecule, which was highly expressed on APCs but not on tumor cells (84.61% ±2.74 vs. 6.48% ±1.98, $p = 0.0003$, n = 8, Fig. 6F). We also detected $CD39^+$ T-cells (15.29% ±4.05, n = 8, Fig. 6F). The tumor–immune cell interactions in the tumor microenvironment are summarized schematically in Fig. 6G.

3.6. The cytokine balance in patients' plasma is anti-inflammatory compared to healthy donors

We examined the concentration of 16 proteins in the patients' and donors' plasma. The concentration of IL-10 was significantly higher in patients' plasma and there was a trend for decreased concentration of IL-2 and IL-12 (Table 4). The concentrations of IL-5, MCP-1 and FasL were significantly lower compared to the healthy donors (Table 4). There was no significant difference in the concentration of other proteins examined (Table 4). Unexpectedly, the mean levels of VEGF in patients and donors were similar, contrary to other studies reporting significant increase of VEGF concentration in the plasma of brain tumor patients (Sciacca et al., 2004). In most cases of both patients and donors, TGFβ plasma levels were undetectable (data not shown).

4. Discussion

The aim of our work was to perform an integrated characterization of GBM patients' immune contexture both within the tumor microenvironment and at the systemic level. All research reports referring to glioma immunity published so far present investigations focused on particular subpopulations and markers. However, simultaneous analysis of the multitude of immune defects in patients may help in designing novel immunotherapies, more individualized treatments and pre-empting possible escape mechanisms.

Contradictory reports exist (Dunn et al., 2007) regarding the prognostic value of immune infiltrates in GBM patients. Several recent studies observed positive correlation of increased numbers of glioma infiltrating lymphocytes with better patients' survival (Yang et al., 2010b; Lohr et al., 2011; Kim et al., 2012), while some older reports describe negative (Safdari et al., 1985) or no correlation (Rossi et al., 1989). These discordances could be related to different approaches used to identify lymphocyte subpopulations. In our study, increased infiltration of $CD3^+$ immune cells in the tumor microenvironment was significantly associated with patients' improved survival, independent of age at diagnosis, MGMT promoter hypermethylation and postoperative treatment. Increased $CD8^+$ immune cell infiltration was also significantly associated with improved survival independent of age at diagnosis but not postoperative treatment, while the level of $CD4^+$ cell infiltrates did not significantly correlate with patient survival. $CD3^+$ and $CD8^+$ cells were prognostic for a very small number of patients and may be argued to lack clinical relevance, however, the association of $CD3^+$ cells with almost double increased lifespan may underlie a very important

Fig. 3. Patients' T-cells are suppressed within the tumor microenvironment and at the systemic level. A. Proportions of CTLs within donors' and patients' peripheral T-cells (n = 9) and tumor infiltrating T-cells (n = 8). B. Proportions of T_h cells within donors' and patients' peripheral T-cells (n = 9) and tumor infiltrating T-cells (n = 8). C and D. Representative histograms showing expression of CD28 on CTLs (C) and T_h cells (D) (CD28 — filled histogram, isotype control — open histogram) and proportions of $CD28^+$ cells within donors' and patients' peripheral (n = 9) and tumor infiltrating (n = 8) CTL cells (C) and T_h cells (D). E. Proportions of $CD62L^+$ cells within donors' and patients' peripheral (n = 9) and tumor infiltrating (n = 8) CTL cells and T_h cells. F. Proportions of $CD56^+$ cells within donors' and patients' peripheral (n = 9) and tumor infiltrating (n = 8) CTLs. G. Proportions of CTLA-4^+ cells within donors' and patients' peripheral (n = 9) and tumor infiltrating (n = 8) T_h cells. H. Gating strategy for naturally occurring T_{regs} in peripheral blood: Gate $CD4^+CD25^{high}$ cells on $CD3^+CD4^+$ (T_h cells) population, then on $CD4^+CD25^{high}$ the $Foxp3^+$ cells (T_{regs}) were gated (filled histograms: Foxp3 expression on $CD4^+CD25^{high}$ cells, open histograms with solid line: isotype control). The T_{regs} population identity was confirmed with the high expression of CTLA-4 and low expression of CD127 (filled histograms: markers' expression on T_{regs}, open histograms with solid line: isotype control, open histogram with dashed line: markers' expression on $CD4^+CD25^-$ population). I. Proportions of T_{regs} within donors' and patients' peripheral T cells (n = 9). J. Representative plots showing $CD8^+CD28^-Foxp3^+$ T_{regs} population present in the GBM biopsy (left) versus isotype control (right). K. Tumor infiltrating NK cells gated as $CD3^-CD56^+$ lymphocytes (left) were predominantly $CD56^{dim}CD16^{dim}$ (right) and expressed NKG2D (bottom).

Table 3
Patients' T cells are suppressed within the tumor microenvironment and at the systemic level. All % values represent mean ± SEM, n — number of cases analyzed.

	Donors' PBMCs (n = 9)	Patients' PBMCs (n = 9)	GBM biopsy (n = 8)	Statistical analysis
% of T_h within T cells	65.68 ± 2.10	45.28 ± 7.2	29.43 ± 3.31	Kruskal–Wallis test: p = 0.0005; Dunn's Multiple Comparison Test: p < 0.05 for donors' PBMCs vs. patients' PBMCs
% of CTLs within T cells	26.32 ± 1.65	37.89 ± 7.05	25.86 ± 2.80	Kruskal–Wallis test: p = 0.2883; Dunn's Multiple Comparison Test: p > 0.05
% of $CD28^+$ cells within CTLs	53.92 ± 7.25	42.60 ± 9.40	9.45 ± 3.70	Kruskal–Wallis test: p = 0.0009; Dunn's Multiple Comparison Test: p < 0.05 for patients' PBMCs vs. GBM biopsy
% of $CD28^+$ cells within T_h	96.36 ± 1.42	90.13 ± 3.60	39.48 ± 8.68	Kruskal–Wallis test: p = 0.0002; Dunn's Multiple Comparison Test: p < 0.05 for patients' PBMCs vs. GBM biopsy
% of $CD62L^+$ cells within CTLs	12.04 ± 2.69	15.03 ± 4.22	0.09 ± 0.09	Kruskal–Wallis test: p = 0.0002; Dunn's Multiple Comparison Test: p < 0.05 for patients' PBMCs vs. GBM biopsy
% of $CD62L^+$ cells within T_h	28.87 ± 5.31	11.49 ± 3.44	0.14 ± 0.14	Kruskal–Wallis test: p = 0.0001; Dunn's Multiple Comparison Test: p < 0.05 for patients' PBMCs vs. GBM biopsy
% of $CD56^+$ cells within CTLs	11.93 ± 2.22	20.78 ± 4.03	4.73 ± 1.54	Kruskal–Wallis test: p = 0.0052; Dunn's Multiple Comparison Test: p < 0.05 for patients' PBMCs vs. GBM biopsy
% of CTLA-4^+ cells within T_h	14.03 ± 1.60	25.63 ± 3.53	18.21 ± 3.91	Kruskal–Wallis test: p = 0.0348; Dunn's Multiple Comparison Test: p < 0.05 for donors' PBMCs vs. patients' PBMCs
% of $CD4^+CD25^{high}Foxp3^+$ T_{regs} within T cells	0.43 ± 0.11	0.34 ± 0.13	Not detected	Wilcoxon signed rank test: p = 0.2859 for donors' PBMCs vs. patients' PBMCs

fundamental function of these immune cells in tumor progression. MGMT promoter methylation was not correlated with patient survival and this can be explained by the relatively small sample size and the fact that we analyzed samples from only one clinical centre. Moreover, the prognostic value of MGMT promoter methylation has been questioned (Costa et al., 2010). Future work will be required to validate

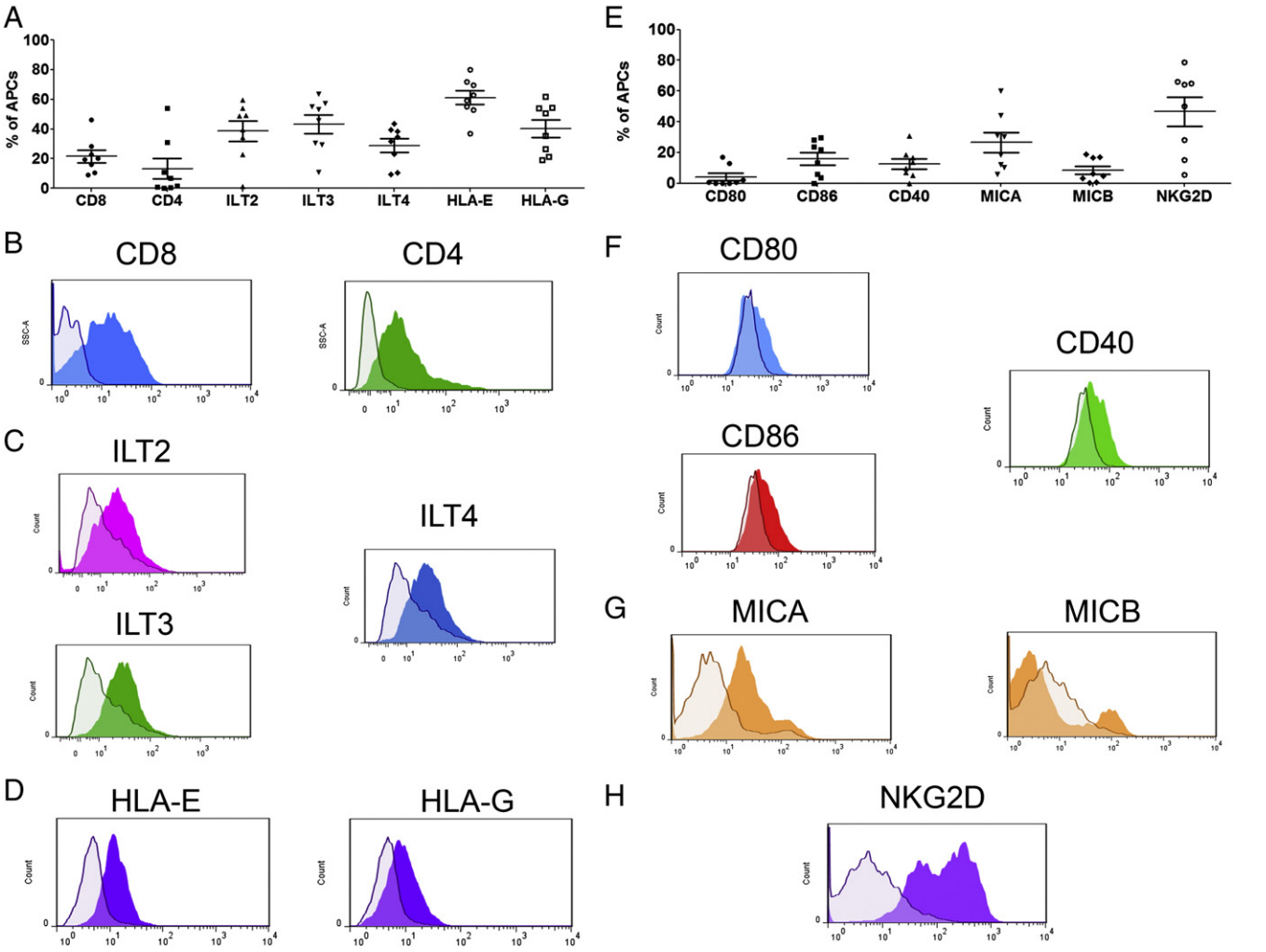

Fig. 4. Tumor infiltrating macrophage/microglia present immunotolerized phenotype. Proportions of APCs expressing CD8, CD4, ILT2,3,4 and HLA-E,G (A), n = 8. Representative histograms showing expression of CD8 and CD4 (B), ILT2,3,4 (C), HLA-E,G (D). Proportions of APCs expressing CD80, CD86, CD40, MICA/B and NKG2D (E), n = 8. Representative histograms showing expression of CD80, CD86, CD40 (F), MICA/B (G), and NKG2D (H) on tumor infiltrating APCs (filled histograms — markers, open histograms — isotype control).

these findings with larger patient cohorts obtained from multicenter clinics. The expression of CD4 and CD8 markers is not restricted to T lymphocytes, but has been also described on monocytes, macrophages and dendritic cells (Gibbings and Befus, 2009). Accordingly, APCs in our patient cohort did express CD4 and CD8. However, since CD3, CD4 and CD8 were strongly correlated, prognostic significance of $CD8^+$ immune cell infiltration is related rather to the CTL subpopulation.

However, since GBM still remains the tumor with the worst prognosis, we hypothesized that the inefficient immune surveillance and response occur due to partially impaired functionality of immune cells recruited to the tumor and/or systemic immunosuppression. The limitation of our study is the lack of functional experiments. However, most aberrations in immune cells functionality are closely related to their phenotype. Therefore, our study is highly relevant for translational research, as it resolves GBM patients' immune status. We observed that smaller proportions of tumor infiltrating T-cells expressed co-stimulatory receptor CD28 and CD56 – an adhesion molecule associated with increased cytotoxicity (Pittet et al., 2000) – compared to those from patients' peripheral blood. This suggests a decreased cytotoxic potential and co-stimulation of tumor infiltrating T-cells. On the other hand, T-cells infiltrating the tumor display a CD62L negative effector phenotype (Yang et al., 2011). The majority of tumor infiltrating CTLs express also the NKG2D activating receptor (Bauer et al., 1999). We observed a decreased proportion of T_h cells within patients' peripheral T-cells. Those cells also expressed higher levels of the inhibitory receptor CTLA-4; however, it tends to decrease within the tumor microenvironment. On the other hand, an increased proportion of patients' T-cells expressed CD56. Therefore, we speculate that T-cells entering the brain are competent, however, once in the tumor microenvironment, they become suppressed and acquire immunotolerant features. Furthermore, we observed down-regulation of co-stimulatory pathways that play critical roles in immunity. Low expression of CD80 and CD86 on APCs and down-regulation of their receptor CD28 on T-cells impairs adaptive immune responses (Smith-Garvin et al., 2009; Ribot et al., 2012). Another co-stimulatory pathway affected in our GBM patients is the absent interaction of CD40 on APCs with its ligand CD154, normally expressed on activated T-cells (Foy et al., 1996; Jyothi and Khar, 2000), but absent in TILs in our GBM patients.

Recently, increasing numbers of reports describe higher proportion and the immunosuppressive action of various T_{regs} subpopulations in the peripheral blood and tumor microenvironment of cancer patients including glioma (Fecci et al., 2006; Heimberger et al., 2008; Sonabend et al., 2008; Wang, 2008; Jacobs et al., 2010). Our results are in contrast with other studies demonstrating an increased proportion of $CD4^+CD25^{high}Foxp3^+$ cells in the peripheral blood and tumor microenvironment of GBM patients (Fecci et al., 2006). This might be explained by the small number of patients we examined, as in the previous reports the increased T_{regs} fraction was not observed for all the patients (Fecci et al., 2006). However, in the tumor microenvironment we detected $CD8^+CD28^-Foxp3^+$ T_{regs} and this finding might explain modest correlation of $CD8^+$ cell infiltrates with patients' outcome. The $CD8^+CD28^-Foxp3^+$ T_{regs} population has been described to be induced by tumor and to mediate the tolerization of DCs and non-professional APCs by up-regulating the expression of inhibitory receptors belonging to the ILT family and down-regulating co-stimulatory molecules CD40, CD80 and CD86 (Wang, 2008; Chui and Li, 2009). Within the tumor infiltrating APCs we observed high expression of ILT2, ILT3 and ILT4 and decreased expression of CD40, CD80 and CD86, thus, we speculate that a $CD8^+CD28^-Foxp3^+$ T_{regs}-mediated immunotolerization occurs in GBM patients. This tumor immune escape mechanism has been reported in other cancers (Cortesini, 2007; Filaci et al., 2007)

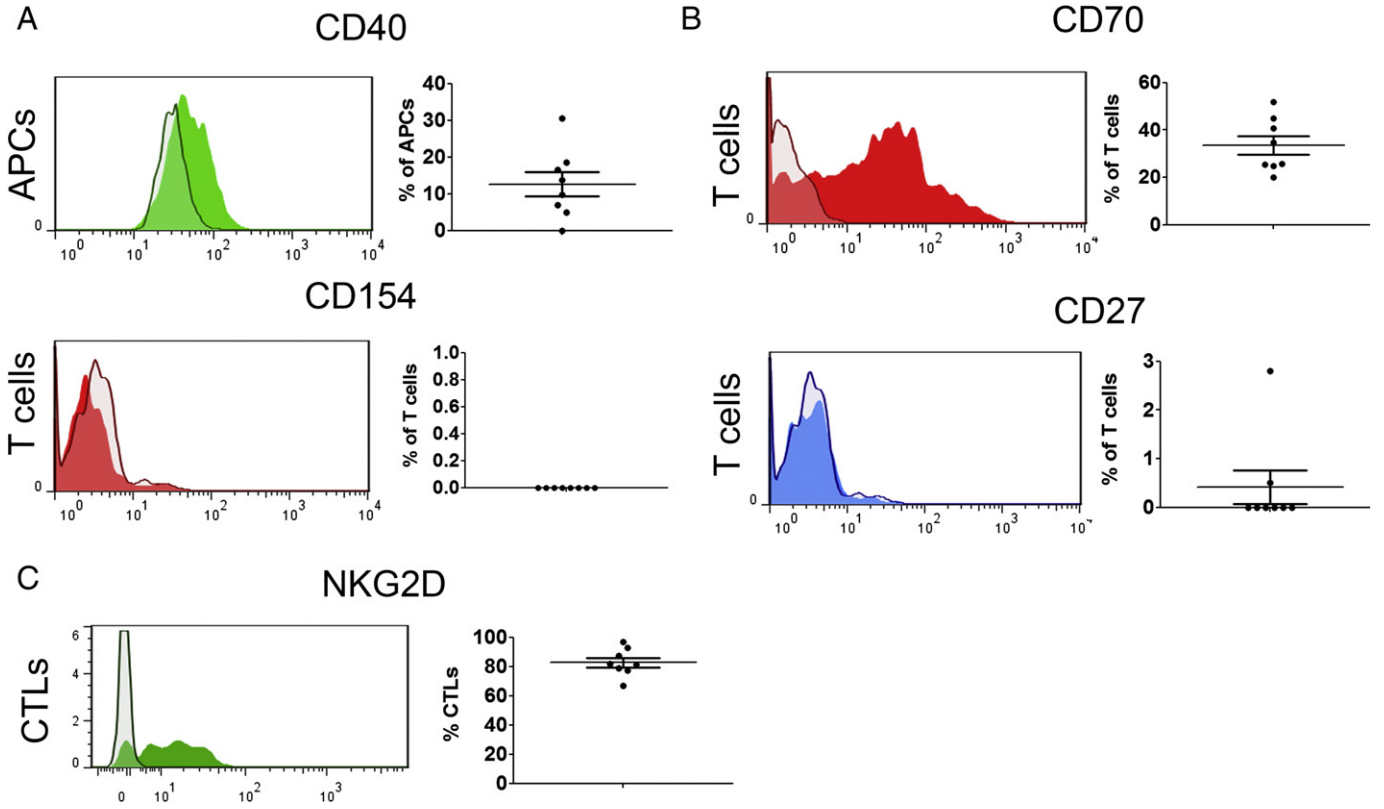

Fig. 5. Tumor infiltrating immune cells display impaired expression of co-stimulatory molecules A. Representative histograms showing expression of CD40 on tumor infiltrating APCs and CD154 on tumor infiltrating T cells and proportions of cells expressing CD40 and CD154 (n = 8). B. Representative histograms showing expression of CD70 and CD27 on tumor infiltrating T-cells and proportions of cells expressing CD70 and CD27 (n = 8). C. Representative histograms showing expression of NKG2D on tumor infiltrating CTLs and proportions of cells expressing NKG2D (n = 8) (filled histograms — markers, open histograms — isotype control).

however it needs further investigation in the context of GBM. Moreover, high proportions of APCs were positive for HLA-E and HLA-G that are ligands for ILT2 and ILT4 (Shiroishi et al., 2003). Furthermore, we show that APCs may support tumor-driven immunosuppression via surface expression of CD39 in addition to CD73 expressed on tumor cells. Ectonucleotidases CD39 and CD73 catalyze two-step degradation of extracellular ATP and ADP. Overexpression of those enzymes has been reported in cancer (Zhang, 2010) and leads to elevated level of extracellular adenosine and T-cell and NK cell suppression (Hausler et al., 2011). Interestingly, the compartmentalization of CD39 and CD73 expression in our GBM patients suggests, that tumor cells adapt to the immune status within tumor microenvironment. On the other hand, a proportion of tumor infiltrating APCs expressed MICA, potentially providing stimulating signal for NK cells through the NKG2D receptor (Kloss et al., 2008; Eissmann et al., 2010). Interestingly, APCs also expressed NKG2D receptor. This has not been reported in

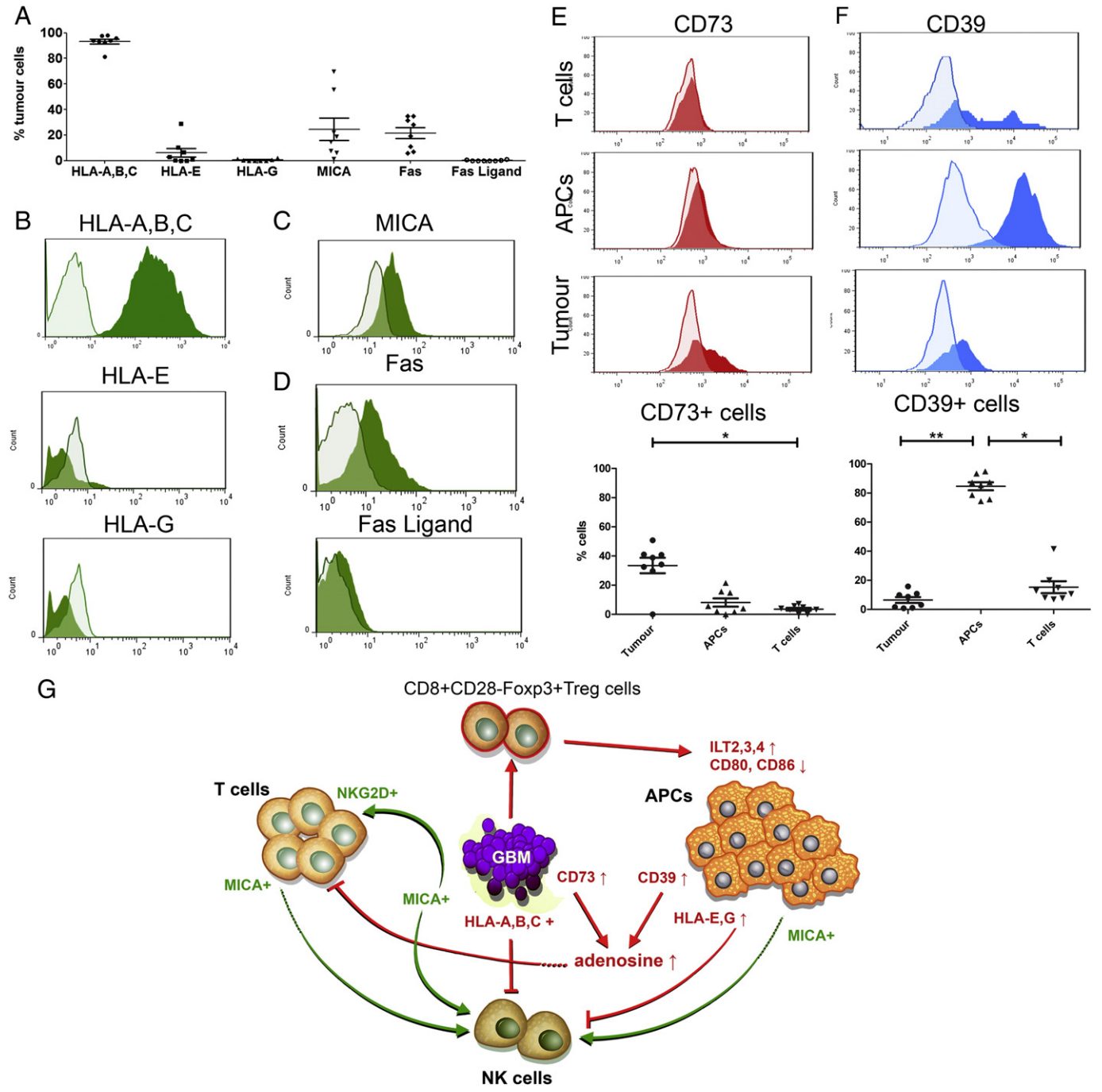

Fig. 6. Tumor integrated mechanisms of immune escape vs. potential immunogenicity. Proportions of tumor cells expressing HLA-A,B,C,E,G, MICA, Fas and FasL, n = 8 (A). Expression on HLA-A,B,C,E,G (B), MICA (C), Fas and FasLigand (D) on tumor cells. Expression of CD39 (E) and CD73 (F) on tumor cells and tumor infiltrating T-cells and APCs and proportions of $CD39^+$ (E) and $CD73^+$ (F) cells within tumor cells and tumor infiltrating T-cells and APCs (n = 8) (filled histograms — markers, open histograms — isotype control) G. Schematic summary of the molecular interactions between the tumor and immune cells in the tumor microenvironment. Red blunt lines indicate inhibition that supports tumor progression, red arrows indicate stimulation of signals that support tumor progression, and green arrows indicate activation signals that inhibit tumor progression.

Table 4
Concentration of selected cytokines and chemokines in GBM patients' plasma compared to healthy donors' (Wilcoxon signed rank test).

Protein (flex set)	Bead position	Mean concentration in donors' plasma [pg/ml] ± SEM, n	Mean concentration in patients' plasma [pg/ml] ± SEM, n	p value
Fas Ligand	C6	24.23 ± 2.633, n = 10	10.76 ± 2.423, n = 10	**0.004**
IL-2	A4	36.61 ± 10.74, n = 10	15.97 ± 6.817, n = 10	0.109
IL-5	A6	5.689 ± 0.7426, n = 10	2.544 ± 1.064, n = 10	**0.042**
IL-10	B7	7.371 ± 1.628, n = 9	21.77 ± 3.877, n = 9	**0.004**
IL-12/IL-23p40	E5	24.79 ± 4.735, n = 10	11.72 ± 4.774, n = 10	0.098
MCP-1	D8	115.8 ± 16.26, n = 10	42.19 ± 6.713, n = 10	**0.002**
Granzyme B	D7	36.99 ± 17.67, n = 8	18.51 ± 11.63, n = 8	0.444
IFNγ	E7	6.283 ± 2.679, n = 10	6.441 ± 2.765, n = 10	1.000
IL-4	A5	7.182 ± 2.370, n = 9	4.488 ± 1.963, n = 9	0.811
IL-6	A7	3.896 ± 1.494 n = 10	3.075 ± 1.343 n = 10	0.813
IL-13	E6	6.505 ± 2.427 n = 10	5.457 ± 1.882 n = 10	1.000
IL-17A	B5	7.296 ± 4.430 n = 9	4.606 ± 4.019 n = 9	0.892
MIP-1α	B9	9.700 ± 5.673 n = 10	3.506 ± 3.506 n = 10	0.375
RANTES	D4	1773 ± 593.3 n = 10	2806 ± 1699 n = 10	0.492
VEGF	B8	17.12 ± 5.121 n = 7	12.09 ± 5.183 n = 7	0.578

The p-values in bold are those that are statistically significant.

human APCs so far, while in rodents it is believed that NKG2D expression on activated macrophages plays an important role in immunity (Diefenbach et al., 2000).

We examined GBM cells for the presence of several surface molecules that are known to activate or inhibit immune cells. Tumor cells are described to be deficient in MHC class I expression and due to that they present potent target for NK cell mediated lysis via "missing self" mechanism (Purdy and Campbell, 2009). To avoid that, they express non-classical MHC class I molecules HLA-E and HLA-G that bind inhibitory receptors on NK cell's surface (Mittelbronn et al., 2007). However, in all patients we analyzed, the majority of tumor cells were positive for HLA-A,B,C that protects them from NK cell-mediated cytotoxicity by binding inhibitory receptors on NK cells (Purdy and Campbell, 2009). On the other hand, tumor cells were negative for HLA-G and HLA-E. NK cells represented 2.11% of all tumor infiltrating immune cells and had $CD56^{dim}CD16^{negative}$ phenotype that was previously reported to represent greater activation in some tumors (Levy et al., 2011). Furthermore upon incubation with tumor target cells, NK cells have been demonstrated to down-regulate CD16 (Grzywacz et al., 2007). We also examined GBM cells for the expression of MICA and MICB — ligands for the activating receptor NKG2D expressed on NK cells and on a subset of CD8 T-cells. All tumor cells were MICB negative, however, some of them expressed MICA, potentially providing stimulating signals to CTLs and NK cells. In addition we found a proportion of tumor cells expressing Fas, thus representing potent target for Fas-mediated apoptosis. Tumor cells did not display FasL surface expression, which has been described to induce apoptosis of tumor infiltrating immune cells (Gomez and Kruse, 2006). These results suggest that GBM is resistant to autologous NK cell-mediated cytotoxicity due to MHC class I expression on the tumor cells. However, HLA-A,B,C expression makes the tumor potentially sensitive to CTL-mediated immune response and our finding of the positive correlation of increased $CD3^+$ and $CD8^+$ infiltration into the tumor with improved patients' survival supports this conclusion. Moreover, due to expression of MICA and absence of HLA-G and HLA-E surface expression, a proportion of tumor cells may be sensitive to allogeneic NK cell with KIR receptor–HLA ligand mismatch.

In addition, our results reveal that the cytokine balance in GBM patients is shifted towards anti-inflammatory profile. IL-10 is an immunosuppressive cytokine, whereas Th1 cytokines induce T-cell maturation into T_{h1} type cells that perform cytotoxic functions and are potentially capable of defending against cancer (Kidd, 2003). It has been described that the cytokine signaling in the periphery and in the brain influences each other (Quan and Herkenham, 2002). In this context, there may be a link between elevated IL-10 in patients' plasma and overexpression of ILT receptors on tumor infiltrating immune cells, as such a correlation has already been suggested (Chui and Li, 2009).

In conclusion, our study showed beneficial role of immune cell infiltration into the tumor in GBM patients, despite multiple mechanisms of tumor immune escape. Our detailed investigation identified potent targets for enhancing immune response and/or overriding tumor-driven immunosuppression. An example of such a target is the inhibitory receptor CTLA-4. Ipilimumab, the anti-CTLA-4 antibody, has already been successfully applied in melanoma patients (Hodi et al., 2010; Robert et al., 2011) and in-vivo studies showed promising results in brain tumor (Fecci et al., 2007). In GBM patients we observed upregulated expression of CTLA-4 in peripheral T_h cells, thus we hypothesize that the therapy targeting this receptor may be also applicable in GBM as an adjuvant treatment.

Supplementary data to this article can be found online at http://dx.doi.org/10.1016/j.jneuroim.2013.08.013.

Authorship

J.K. performed the experiments, analyzed and interpreted data and wrote the manuscript; A.P. and N.H.C.B. contributed to experimental design, data analysis and manuscript editing; J.Z. contributed to data interpretation and manuscript editing; GE performed multivariate Cox regression analysis, AW performed MGMT bisulfite pyrosequencing and data analysis; PØE obtained clinical information, provided access to the patient biobank and contributed to data interpretation; and M.C. designed the research and contributed to data analysis and interpretation, manuscript writing and provided funding.

Conflict of interest

The authors have no competing financial interests.

Acknowledgements

We thank the GBM patients and voluntary healthy donors that consented to donating their blood and tumor tissue for use in this research. This work was supported by The Norwegian Cancer Society (PK01-2008-0093), The Meltzer Fond, The Norwegian Research Council FRIFORSK and The Bergen Medical Research Foundation. We also thank The National Genome Research Network NGFNplus, Brain Tumor Net (grant 01GS08187, SP8), of the German Ministry for Education and Research for their support. We are grateful to Bodil B. Hansen, Tove Johannsen, and Ingrid Gravdal for technical assistance. We thank Professor Rolf Bjerkvig for providing the laboratory infrastructure where our research was performed. Flow cytometric analyses were performed at Centre de Recherche Public de la Santé, Luxembourg and at the Molecular Imaging Centre, University of Bergen, supported by the National Program for Research in Functional Genomics (FUGE), funded by the Norwegian Research Council.

References

Alter, A., Duddy, M., Hebert, S., Biernacki, K., Prat, A., Antel, J.P., Yong, V.W., Nuttall, R.K., Pennington, C.J., Edwards, D.R., Bar-Or, A., 2003. Determinants of human B cell migration across brain endothelial cells. J. Immunol. 170, 4497–4505.

Bauer, S., Groh, V., Wu, J., Steinle, A., Phillips, J.H., Lanier, L.L., Spies, T., 1999. Activation of NK cells and T cells by NKG2D, a receptor for stress-inducible MICA. Science 285, 727–729.

Becher, B., Prat, A., Antel, J.P., 2000. Brain–immune connection: immuno-regulatory properties of CNS-resident cells. Glia 29, 293–304.

Carpentier, A.F., Meng, Y., 2006. Recent advances in immunotherapy for human glioma. Curr. Opin. Oncol. 18, 631–636.

Chui, C.S., Li, D., 2009. Role of immunoglobulin-like transcript family receptors and their ligands in suppressor T-cell-induced dendritic cell tolerization. Hum. Immunol. 70, 686–691.

Cortesini, R., 2007. Pancreas cancer and the role of soluble immunoglobulin-like transcript 3 (ILT3). JOP 8, 697–703.

Costa, B.M., Caeiro, C., Guimaraes, I., Martinho, O., Jaraquemada, T., Augusto, I., Castro, L., Osorio, L., Linhares, P., Honavar, M., Resende, M., Braga, F., Silva, A., Pardal, F., Amorim, J., Nabico, R., Almeida, R., Alegria, C., Pires, M., Pinheiro, C., Carvalho, E., Lopes, J.M., Costa, P., Damasceno, M., Reis, R.M., 2010. Prognostic value of MGMT promoter methylation in glioblastoma patients treated with temozolomide-based chemoradiation: a Portuguese multicentre study. Oncol. Rep. 23, 1655–1662.

Costello, R.T., Sivori, S., Mallet, F., Sainty, D., Arnoulet, C., Reviron, D., Gastaut, J.A., Moretta, A., Olive, D., 2002. A novel mechanism of antitumor response involving the expansion of CD3+/CD56+ large granular lymphocytes triggered by a tumor-expressed activating ligand. Leuk. Off. J. Leuk. Soc. Am. Leuk. Res. Fund UK 16, 855–860.

de Visser, K.E., Eichten, A., Coussens, L.M., 2006. Paradoxical roles of the immune system during cancer development. Nat. Rev. Cancer 6, 24–37.

Diefenbach, A., Jamieson, A.M., Liu, S.D., Shastri, N., Raulet, D.H., 2000. Ligands for the murine NKG2D receptor: expression by tumor cells and activation of NK cells and macrophages. Nat. Immunol. 1, 119–126.

Dunn, G.P., Dunn, I.F., Curry, W.T., 2007. Focus on TILs: prognostic significance of tumor infiltrating lymphocytes in human glioma. Cancer Immun. 7, 12.

Eissmann, P., Evans, J.H., Mehrabi, M., Rose, E.L., Nedvetzki, S., Davis, D.M., 2010. Multiple mechanisms downstream of TLR-4 stimulation allow expression of NKG2D ligands to facilitate macrophage/NK cell crosstalk. J. Immunol. 184, 6901–6909.

Fecci, P.E., Mitchell, D.A., Whitesides, J.F., Xie, W., Friedman, A.H., Archer, G.E., Herndon II, J.E., Bigner, D.D., Dranoff, G., Sampson, J.H., 2006. Increased regulatory T-cell fraction amidst a diminished CD4 compartment explains cellular immune defects in patients with malignant glioma. Cancer Res. 66, 3294–3302.

Fecci, P.E., Ochiai, H., Mitchell, D.A., Grossi, P.M., Sweeney, A.E., Archer, G.E., Cummings, T., Allison, J.P., Bigner, D.D., Sampson, J.H., 2007. Systemic CTLA-4 blockade ameliorates glioma-induced changes to the CD4+ T cell compartment without affecting regulatory T-cell function. Clin. Cancer Res. 13, 2158–2167.

Filaci, G., Fenoglio, D., Fravega, M., Ansaldo, G., Borgonovo, G., Traverso, P., Villaggio, B., Ferrera, A., Kunkl, A., Rizzi, M., Ferrera, F., Balestra, P., Ghio, M., Contini, P., Setti, M., Olive, D., Azzarone, B., Carmignani, G., Ravetti, J.L., Torre, G., Indiveri, F., 2007. CD8+ CD28-T regulatory lymphocytes inhibiting T cell proliferative and cytotoxic functions infiltrate human cancers. J. Immunol. 179, 4323–4334.

Foy, T.M., Aruffo, A., Bajorath, J., Buhlmann, J.E., Noelle, R.J., 1996. Immune regulation by CD40 and its ligand GP39. Annu. Rev. Immunol. 14, 591–617.

Garcia, P., De Heredia, A.B., Bellon, T., Carpio, E., Llano, M., Caparros, E., Aparicio, P., Lopez-Botet, M., 2004. Signalling via CD70, a member of the TNF family, regulates T cell functions. J. Leukoc. Biol. 76, 263–270.

Gibbings, D., Befus, A.D., 2009. CD4 and CD8: an inside–out coreceptor model for innate immune cells. J. Leukoc. Biol. 86, 251–259.

Gomez, G.G., Kruse, C.A., 2006. Mechanisms of malignant glioma immune resistance and sources of immunosuppression. Gene Ther. Mol. Biol. 10, 133–146.

Grzywacz, B., Kataria, N., Verneris, M.R., 2007. CD56(dim)CD16(+) NK cells downregulate CD16 following target cell induced activation of matrix metalloproteinases. Leukemia 21, 356–359 (author reply 359).

Hartigan-O'Connor, D.J., Poon, C., Sinclair, E., McCune, J.M., 2007. Human CD4+ regulatory T cells express lower levels of the IL-7 receptor alpha chain (CD127), allowing consistent identification and sorting of live cells. J. Immunol. Methods 319, 41–52.

Hausler, S.F., Montalban del Barrio, I., Strohschein, J., Anoop Chandran, P., Engel, J.B., Honig, A., Ossadnik, M., Horn, E., Fischer, B., Krockenberger, M., Heuer, S., Seida, A.A., Junker, M., Kneitz, H., Kloor, D., Klotz, K.N., Dietl, J., Wischhusen, J., 2011. Ectonucleotidases CD39 and CD73 on OvCA cells are potent adenosine-generating enzymes responsible for adenosine receptor 2A-dependent suppression of T cell function and NK cell cytotoxicity. Cancer Immunol. Immunother.: CII 60, 1405–1418.

Hegi, M.E., Diserens, A.C., Gorlia, T., Hamou, M.F., de Tribolet, N., Weller, M., Kros, J.M., Hainfellner, J.A., Mason, W., Mariani, L., Bromberg, J.E., Hau, P., Mirimanoff, R.O., Cairncross, J.G., Janzer, R.C., Stupp, R., 2005. MGMT gene silencing and benefit from temozolomide in glioblastoma. N. Engl. J. Med. 352, 997–1003.

Heimberger, A.B., Abou-Ghazal, M., Reina-Ortiz, C., Yang, D.S., Sun, W., Qiao, W., Hiraoka, N., Fuller, G.N., 2008. Incidence and prognostic impact of FoxP3+ regulatory T cells in human gliomas. Clin. Cancer Res. 14, 5166–5172.

Hodi, F.S., O'Day, S.J., McDermott, D.F., Weber, R.W., Sosman, J.A., Haanen, J.B., Gonzalez, R., Robert, C., Schadendorf, D., Hassel, J.C., Akerley, W., van den Eertwegh, A.J., Lutzky, J., Lorigan, P., Vaubel, J.M., Linette, G.P., Hogg, D., Ottensmeier, C.H., Lebbe, C., Peschel, C., Quirt, I., Clark, J.I., Wolchok, J.D., Weber, J.S., Tian, J., Yellin, M.J., Nichol, G.M., Hoos, A., Urba, W.J., 2010. Improved survival with ipilimumab in patients with metastatic melanoma. N. Engl. J. Med. 363, 711–723.

Jacobs, J.F., Idema, A.J., Bol, K.F., Grotenhuis, J.A., de Vries, I.J., Wesseling, P., Adema, G.J., 2010. Prognostic significance and mechanism of Treg infiltration in human brain tumors. J. Neuroimmunol. 225, 195–199.

Jeffes III, E.W., Beamer, Y.B., Jacques, S., Silberman, R.S., Vayuvegula, B., Gupta, S., Coss, J.S., Yamamoto, R.S., Granger, G.A., 1993. Therapy of recurrent high grade gliomas with surgery, and autologous mitogen activated IL-2 stimulated killer (MAK) lymphocytes: I. Enhancement of MAK lytic activity and cytokine production by PHA and clinical use of PHA. J. Neurooncol. 15, 141–155.

Jyothi, M.D., Khar, A., 2000. Regulation of CD40L expression on natural killer cells by interleukin-12 and interferon gamma: its role in the elicitation of an effective antitumor immune response. Cancer Immunol. Immunother. CII 49, 563–572.

Kaplan, E.L., Meier, P., 1958. Nonparametric estimation from incomplete observations. J. Am. Stat. Assoc. 53, 457–481.

Kidd, P., 2003. Th1/Th2 balance: the hypothesis, its limitations, and implications for health and disease. Altern. Med. Rev. 8, 223–246.

Kim, Y.H., Jung, T.Y., Jung, S., Jang, W.Y., Moon, K.S., Kim, I.Y., Lee, M.C., Lee, J.J., 2012. Tumour-infiltrating T-cell subpopulations in glioblastomas. Br. J. Neurosurg. 26, 21–27.

Kloss, M., Decker, P., Baltz, K.M., Baessler, T., Jung, G., Rammensee, H.G., Steinle, A., Krusch, M., Salih, H.R., 2008. Interaction of monocytes with NK cells upon Toll-like receptor-induced expression of the NKG2D ligand MICA. J. Immunol. 181, 6711–6719.

Levy, E.M., Roberti, M.P., Mordoh, J., 2011. Natural killer cells in human cancer: from biological functions to clinical applications. J. Biomed. Biotechnol. 2011, 676198.

Lohr, J., Ratliff, T., Huppertz, A., Ge, Y., Dictus, C., Ahmadi, R., Grau, S., Hiraoka, N., Eckstein, V., Ecker, R.C., Korff, T., von Deimling, A., Unterberg, A., Beckhove, P., Herold-Mende, C., 2011. Effector T-cell infiltration positively impacts survival of glioblastoma patients and is impaired by tumor-derived TGF-beta. Clin. Cancer Res. 17, 4296–4308.

Louis, D.N., Ohgaki, H., Wiestler, O.D., Cavenee, W.K., Burger, P.C., Jouvet, A., Scheithauer, B.W., Kleihues, P., 2007. The 2007 WHO classification of tumours of the central nervous system. Acta Neuropathol. 114, 97–109.

Malmberg, K.J., Ljunggren, H.G., 2006. Escape from immune- and nonimmune-mediated tumor surveillance. Semin. Cancer Biol. 16, 16–31.

Mantel, N., 1966. Evaluation of survival data and two new rank order statistics arising in its consideration. Cancer Chemother. Rep. 50, 163–170.

Mikeska, T., Bock, C., El-Maarri, O., Hubner, A., Ehrentraut, D., Schramm, J., Felsberg, J., Kahl, P., Buttner, R., Pietsch, T., Waha, A., 2007. Optimization of quantitative MGMT promoter methylation analysis using pyrosequencing and combined bisulfite restriction analysis. J. Mol. Diagn. 9, 368–381.

Mittelbronn, M., Simon, P., Loffler, C., Capper, D., Bunz, B., Harter, P., Schlaszus, H., Schleich, A., Tabatabai, G., Goeppert, B., Meyermann, R., Weller, M., Wischhusen, J., 2007. Elevated HLA-E levels in human glioblastomas but not in grade I to III astrocytomas correlate with infiltrating CD8+ cells. J. Neuroimmunol. 189, 50–58.

Ostrand-Rosenberg, S., Sinha, P., 2009. Myeloid-derived suppressor cells: linking inflammation and cancer. J. Immunol. 182, 4499–4506.

Pittet, M.J., Speiser, D.E., Valmori, D., Cerottini, J.C., Romero, P., 2000. Cutting edge: cytolytic effector function in human circulating CD8+ T cells closely correlates with CD56 surface expression. J. Immunol. 164, 1148–1152.

Prendergast, C.T., Anderton, S.M., 2009. Immune cell entry to central nervous system—current understanding and prospective therapeutic targets. Endocr. Metab. Immune Disord. Drug Targets 9, 315–327.

Purdy, A.K., Campbell, K.S., 2009. Natural killer cells and cancer: regulation by the killer cell Ig-like receptors (KIR). Cancer Biol. Ther. 8, 2211–2220.

Quan, N., Herkenham, M., 2002. Connecting cytokines and brain: a review of current issues. Histol. Histopathol. 17, 273–288.

Ribot, J.C., Debarros, A., Mancio-Silva, L., Pamplona, A., Silva-Santos, B., 2012. B7-CD28 costimulatory signals control the survival and proliferation of murine and human gammadelta T cells via IL-2 production. J. Immunol. 189, 1202–1208.

Robert, C., Thomas, L., Bondarenko, I., O'Day, S., Weber, J., Garbe, C., Lebbe, C., Baurain, J.F., Testori, A., Grob, J.J., Davidson, N., Richards, J., Maio, M., Hauschild, A., Miller Jr., W.H., Gascon, P., Lotem, M., Harmankaya, K., Ibrahim, R., Francis, S., Chen, T.T., Humphrey, R., Hoos, A., Wolchok, J.D., 2011. Ipilimumab plus dacarbazine for previously untreated metastatic melanoma. N. Engl. J. Med. 364, 2517–2526.

Rossi, M.L., Jones, N.R., Candy, E., Nicoll, J.A., Compton, J.S., Hughes, J.T., Esiri, M.M., Moss, T.H., Cruz-Sanchez, F.F., Coakham, H.B., 1989. The mononuclear cell infiltrate compared with survival in high-grade astrocytomas. Acta Neuropathol. 78, 189–193.

Rouas-Freiss, N., Moreau, P., Ferrone, S., Carosella, E.D., 2005. HLA-G proteins in cancer: do they provide tumor cells with an escape mechanism? Cancer Res. 65, 10139–10144.

Safdari, H., Hochberg, F.H., Richardson Jr., E.P., 1985. Prognostic value of round cell (lymphocyte) infiltration in malignant gliomas. Surg. Neurol. 23, 221–226.

Sciacca, F.L., Ciusani, E., Silvani, A., Corsini, E., Frigerio, S., Pogliani, S., Parati, E., Croci, D., Boiardi, A., Salmaggi, A., 2004. Genetic and plasma markers of venous thromboembolism in patients with high grade glioma. Clin. Cancer Res. 10, 1312–1317.

Sehgal, A., Berger, M.S., 2000. Basic concepts of immunology and neuroimmunology. Neurosurg. Focus. 9, e1.

Shiroishi, M., Tsumoto, K., Amano, K., Shirakihara, Y., Colonna, M., Braud, V.M., Allan, D.S., Makadzange, A., Rowland-Jones, S., Willcox, B., Jones, E.Y., van der Merwe, P.A., Kumagai, I., Maenaka, K., 2003. Human inhibitory receptors Ig-like transcript 2 (ILT2) and ILT4 compete with CD8 for MHC class I binding and bind preferentially to HLA-G. Proc. Natl. Acad. Sci. U. S. A. 100, 8856–8861.

Smith-Garvin, J.E., Koretzky, G.A., Jordan, M.S., 2009. T cell activation. Annu. Rev. Immunol. 27, 591–619.

Sonabend, A.M., Rolle, C.E., Lesniak, M.S., 2008. The role of regulatory T cells in malignant glioma. Anticancer. Res. 28, 1143–1150.

Stupp, R., Mason, W.P., van den Bent, M.J., Weller, M., Fisher, B., Taphoorn, M.J., Belanger, K., Brandes, A.A., Marosi, C., Bogdahn, U., Curschmann, J., Janzer, R.C., Ludwin, S.K., Gorlia, T., Allgeier, A., Lacombe, D., Cairncross, J.G., Eisenhauer, E., Mirimanoff, R.O., 2005. Radiotherapy plus concomitant and adjuvant temozolomide for glioblastoma. N. Engl. J. Med. 352, 987–996.

Stupp, R., Hegi, M.E., Mason, W.P., van den Bent, M.J., Taphoorn, M.J., Janzer, R.C., Ludwin, S.K., Allgeier, A., Fisher, B., Belanger, K., Hau, P., Brandes, A.A., Gijtenbeek, J., Marosi, C.,

Vecht, C.J., Mokhtari, K., Wesseling, P., Villa, S., Eisenhauer, E., Gorlia, T., Weller, M., Lacombe, D., Cairncross, J.G., Mirimanoff, R.O., 2009. Effects of radiotherapy with concomitant and adjuvant temozolomide versus radiotherapy alone on survival in glioblastoma in a randomised phase III study: 5-year analysis of the EORTC-NCIC trial. Lancet Oncol. 10, 459–466.

Tang, J., Flomenberg, P., Harshyne, L., Kenyon, L., Andrews, D.W., 2005. Glioblastoma patients exhibit circulating tumor-specific CD8+ T cells. Clin. Cancer Res. 11, 5292–5299.

Ueda, R., Low, K.L., Zhu, X., Fujita, M., Sasaki, K., Whiteside, T.L., Butterfield, L.H., Okada, H., 2007. Spontaneous immune responses against glioma-associated antigens in a long term survivor with malignant glioma. J. Transl. Med. 5, 68.

Wang, R.F., 2008. CD8+ regulatory T cells, their suppressive mechanisms, and regulation in cancer. Hum. Immunol. 69, 811–814.

Yang, I., Han, S.J., Kaur, G., Crane, C., Parsa, A.T., 2010a. The role of microglia in central nervous system immunity and glioma immunology. J. Clin. Neurosci. 17, 6–10.

Yang, I., Tihan, T., Han, S.J., Wrensch, M.R., Wiencke, J., Sughrue, M.E., Parsa, A.T., 2010b. CD8+ T-cell infiltrate in newly diagnosed glioblastoma is associated with long-term survival. J. Clin. Neurosci. 17, 1381–1385.

Yang, S., Liu, F., Wang, Q.J., Rosenberg, S.A., Morgan, R.A., 2011. The shedding of CD62L (L-selectin) regulates the acquisition of lytic activity in human tumor reactive T lymphocytes. PLoS One 6, e22560.

Zhang, B., 2010. CD73: a novel target for cancer immunotherapy. Cancer Res. 70, 6407–6411.

Zou, J.P., Morford, L.A., Chougnet, C., Dix, A.R., Brooks, A.G., Torres, N., Shuman, J.D., Coligan, J.E., Brooks, W.H., Roszman, T.L., Shearer, G.M., 1999. Human glioma-induced immunosuppression involves soluble factor(s) that alters monocyte cytokine profile and surface markers. J. Immunol. 162, 4882–4892.